Activation of endogenous TRPV1 fails to induce overstimulation-based cytotoxicity in breast and prostate cancer cells but not in pain-sensing neurons

CrossMark

László Pecze [a,*], Katalin Jósvay [b], Walter Blum [a], György Petrovics [c], Csaba Vizler [b], Zoltán Oláh [d,e,1], Beat Schwaller [a,1]

[a] Anatomy, Department of Medicine, University of Fribourg, Route Albert-Gockel 1, Fribourg CH-1700, Switzerland
[b] Institute of Biochemistry, Biological Research Center of the Hungarian Academy of Sciences, Temesvári krt. 62, Szeged H-6701, Hungary
[c] Department of Surgery, Center for Prostate Disease Research, Uniformed Services University of the Health Sciences, Bethesda, MD 20814, USA
[d] Acheuron Hungary Ltd., Szeged H-6726, Hungary [e] Institute of Chemistry, Faculty of Material Science and Engineering, University of Miskolc, H-3515, Hungary
[e] Institute of Chemistry, Faculty of Material Science and Engineering, University of Miskolc, H-3515, Hungary

ARTICLE INFO

ABSTRACT

Vanilloids including capsaicin and resiniferatoxin are potent transient receptor potential vanilloid type 1 (TRPV1) agonists. TRPV1 overstimulation selectively ablates capsaicin-sensitive sensory neurons in animal models in vivo. The cytotoxic mechanisms are based on strong Na^+ and Ca^{2+} influx via TRPV1 channels, which leads to mitochondrial Ca^{2+} accumulation and necrotic cell swelling. Increased TRPV1 expression levels are also observed in breast and prostate cancer and derived cell lines. Here, we examined whether potent agonist-induced overstimulation mediated by TRPV1 might represent a means for the eradication of prostate carcinoma (PC-3, Du 145, LNCaP) and breast cancer (MCF7, MDA-MB-231, BT-474) cells in vitro. While rat sensory neurons were highly vanilloid-sensitive, normal rat prostate epithelial cells were resistant in vivo. We found TRPV1 to be expressed in all cancer cell lines at mRNA and protein levels, yet protein expression levels were significantly lower compared to sensory neurons. Treatment of all human carcinoma cell lines with capsaicin didn't lead to overstimulation cytotoxicity in vitro. We assume that the low vanilloid-sensitivity of prostate and breast cancer cells is associated with low expression levels of TRPV1, since ectopic TRPV1 expression rendered them susceptible to the cytotoxic effect of vanilloids evidenced by plateau-type Ca^{2+} signals, mitochondrial Ca^{2+} accumulation and Na^+- and Ca^{2+}-dependent membrane disorganization. Moreover, long-term monitoring revealed that merely the ectopic expression of TRPV1 stopped cell proliferation and often induced apoptotic processes via strong activation of caspase-3 activity. Our results indicate that specific targeting of TRPV1 function remains a putative strategy for cancer treatment.

1. Introduction

Transient receptor potential vanilloid type 1 (TRPV1) is one of the main pain-sensing receptors in sensory neurons [1,2]. Upon opening, Na^+ and Ca^{2+} ions enter the cytoplasmic compartment through TRPV1 channels localized in the plasma membrane [3]. The channel is activated by elevated temperature (>43 °C) [3], both acidic and basic pH [4], or by endogenous and exogenous compounds. Endogenous agonists such as lipoxygenase products are produced by the body and

bind to and activate the receptor. Exogenous agonists include natural products from e.g. plants (capsaicin (CAPS) from chili pepper and resiniferatoxin (RTX) from a tropical plant called *Euphorbia resinifera*, respectively), but also synthetically produced chemicals.

TRPV1 is mainly expressed in a subset of sensory neurons of the peripheral nerve system [5]. Sensory neurons with their cell bodies located in the trigeminal ganglion (TG) or in the dorsal root ganglion (DRG) convey somatic sensory information from peripheral tissues to the central nervous system. Neurons that express TRPV1 primarily transmit noxious heat or inflammatory pain sensations, while TRPV1 is minimally expressed or absent in motor neurons and non-nociceptive sensory pathways [6]. Besides of sensory neurons, TRPV1 expression was detected in various organs including brain, kidney, lung, testis, pancreas, spleen, liver, stomach, skin, muscle and moreover in cell lines

derived from those tissues [7–9]. It was also reported that several types of normal epithelial cells including bronchial [10], prostate [11] and intestinal [12] epithelial cells express TRPV1 channels, albeit at rather low expression levels. Human keratinocytes show much lower TRPV1 expression levels than neurons within human sensory ganglia and are resistant to vanilloid-induced cytotoxicity [13] suggesting that CAPS and other TRPV1 agonists act differently on peripheral nerves and on keratinocytes. Keratinocytes show negative or weak TRPV1 immuno-staining enmeshed by strongly immuno-positive nerve endings [14]. Functional CAPS-sensitive TRPV1 receptors have been identified in the normal epithelial cells of the urothelium of the urinary bladder; TRPV1 knockout mice exhibit diminished nitric oxide and stretch-evoked adenosine triphosphate release from cells of the urothelium [15]. Despite of the reported widespread expression TRPV1, Cre-recombinase expression driven by the TRPV1 promoter was mostly restricted to peripheral neurons in transgenic mice [16].

The naturally occurring pungent compounds CAPS and RTX acting as TRPV1 agonists [3], when applied at high doses are ablative agents for pain-sensing neurons within DRG and TG of the peripheral nerve system [17]. Abundant expression on pain-sensing neurons renders TRPV1 an excellent novel target in sensory ganglia to manage severe pain conditions without the narcotic side effects of morphine. For "molecular surgery", RTX, the most potent and selective agonist of TRPV1 is used. A number of different routes of applications in rodents, dogs and monkeys were examined, in order to develop a proof-of-concept that TRPV1-specific cell deletion is feasible in the clinic [18–21]. Both robust Na^+ influx across the plasma membrane [22] and Ca^{2+} accumulation first in the cytosol, then in mitochondria [23, 24] are associated with TRPV1-mediated cytotoxicity. The molecular mechanism of TRPV1-mediated cytotoxicity shows conspicuous similarity to glutamate-receptor mediated excitotoxicity [25,26], i.e. robust Na^+ and Ca^{2+} influx, cell swelling, mitochondrial Ca^{2+} loading and production of reactive oxygen species (ROS). Both types of toxicity are essentially based on receptor overstimulation, i.e. an agonist overdose-induced irreversible cellular damage mediated by non-selective cation channels.

The presence of TRPV1 has already been demonstrated in some breast and prostate cancer derived cell lines: LNCaP [11], PC-3 [11] and MCF7 [27–29]. Augmented expression of TRPV1 was reported to correlate with increasing tumor grade in prostate cancers [30]. Up-regulation of TRPV1 channels in neoplastic breast and prostate tissue compared to normal tissue has been reported previously [30–32].

In this study, the effects of TRPV1 overstimulation was investigated in rat prostate glands in vivo, in prostate and breast cancer cell lines, as well as in cultured rat sensory neurons in vitro. We also tested the feasibility of the overstimulation-based cell ablation method for TRPV1-expressing breast and prostate cancer cells.

2. Materials and methods

2.1. Chemicals

CAPS, a TRPV1 agonist, thapsigargin, a sarco/endoplasmic reticulum Ca^{2+}-ATPase pump inhibitor, and the Ca^{2+} ionophore ionomycin (IONO) were dissolved in DMSO (all from Sigma-Aldrich, St. Louis, MO). RTX from the LC Laboratories (Woburn, MA) was dissolved in ethanol at a concentration of 2 mg/ml and further diluted in double distilled water. The final concentration of the solvents (DMSO, ethanol) were <0.1% in all experimental solutions. At these concentrations the solvents did not modify the evoked Ca^{2+} responses and cell viability in control experiments (data not shown). Ethylene glycol tetra acetic acid (EGTA) was dissolved with NaOH in double distilled water at basic pH (pH > 8.0) and then the pH was adjusted to 7.4 with HCl. Propidium iodide was dissolved in double distilled water to yield a 200 mM stock solution.

2.2. Plasmids

The cDNA of the human TRPV1 channel was amplified from RNA isolated from human trigeminal ganglion tissue. Total RNA was isolated with Trizol reagent (Invitrogen), and first strand cDNAs were synthetized with the RevertAid™ H Minus First Strand cDNA Synthesis Kit (Fermentas). The human TRPV1 cDNA was then amplified with Pfu DNA polymerase (Fermentas) with specific forward and reverse primers, 5′-GAG GAT CCA GCA AGG ATG AAG AAA TGG AG-3′ and 5′-GAA TTC AAG GCC CAG TGT TGA CAGTG-3′, respectively. The fragment was then cloned into the BglII and EcoRI sites of the pEGFP-C3 vector (Clontech, Mountain View, CA) and the sequence was verified. The plasmid was named as pGFP-TRPV1. To obtain an untagged version of the TRPV1 channel, the plasmid was digested with Eco47III (blunt end) and ScaI (blunt end) and re-ligated afterwards. This results in the elimination of the cDNA part coding for the EGFP tag. The plasmid was named as pTRPV1.

2.3. Human biopsies and cell lines

Laser captured micro-dissection (LCM) from prostate biopsies was performed in the Department of Surgery, Uniformed Services University of the Health Sciences, Bethesda, MA, USA. All patient samples were collected with informed consent as approved by their respective institutional review boards. Human trigeminal ganglia were dissected from a cadaver. The procedure was approved by the Medical Science and Research Ethics Committee of the University of Szeged in accordance with Hungarian laws (1997th CLIV Law on Health Care) with the ethical approval of the Hungarian Scientific and Research Ethics Committee of the Medical Research Council. Human prostate (PC-3, LNCaP, Du 145) and breast (MCF7, BT-474, MDA-MB-231) cancer cell lines were purchased from ATCC (Manassas, VA, USA). In some experiments, levels of TRPV1 expression were increased in cell lines by overexpression of TRPV1 or of the fusion protein TRPV1-GFP. Transfections of all cell lines with plasmids encoding the cDNA for either TRPV1 or GFP-TRPV1 were performed using the TransIT®-LT1 Transfection Reagent (Mirus, Labforce, Muttenz, Switzerland) according to the manufacturer's instructions. Cell lines overexpressing TRPV1 channels were marked as "cell line name[TRPV1]" or "cell line name[GFP-TRPV1]". DRG primary cultures were prepared from E15 rat embryos. Embryos were removed from the uterus and placed in Petri dishes containing Krebs-Ringer buffer (in mM: NaCl 119, KCl 4.7, $CaCl_2$ 2.5, $MgSO_4$ 1.2, KH_2PO_4 1.2, $NaHCO_3$ 25, glucose 2; pH 7.4). The cords were dissected and DRGs were removed. The tissue was digested in 0.05% trypsin solution at 37 °C for 10 min and dissociated cell cultures were maintained in DMEM containing 5% horse serum and 100 ng/ml nerve growth factor (Sigma-Aldrich) to promote neuronal survival and differentiation. After 2 days in vitro primary DRG cultures were used for the experiments. The human keratinocyte cell line permanently overexpressing TRPV1 receptor (HaCaT[TRPV1]) was established using G418 selection method as described earlier [13].

2.4. Detection of TRPV1 transcript in human biopsies and in breast and prostate carcinoma cell lines

Prostate epithelial cells with either normal or tumor morphology (10–20 cells) were captured from frozen prostate sections of radical prostatectomy specimens with a laser-capture micro-dissection (LCM) instrument (2000 laser shots for one sample). Total RNA was isolated from LCM samples with the MicroRNA kit (Stratagene, La Jolla, CA). The purified mRNA was quantified using RiboGreen dye (Molecular Probes, Eugene, OR) and a VersaFluor fluorimeter (BioRad, Hercules, CA). Isolated RNA was reverse-transcribed with RevertAid™ H Minus First Strand cDNA Synthesis Kit (Fermentas, Waltham, MA). Due to low levels of RNA transcripts from LCM dissected samples, the number of PCR cycles was set to 40, annealing was performed at 65 °C and

30 s were given for extension of the DNA fragments with human TRPV1-specific primer pairs producing a 194 bp product: 5′-GCA CCC TGA GCT TCT CCC TGC GGT CAA-3′ and 5′-GGA AGC GGC AGG ACT CTT GAA GA-3′. As a control for RNA specificity of the amplicon, the RT enzyme was omitted in parallel reactions. Specific fragments formed in the PCR indicated that the reverse transcriptase enzyme was required to convert the specific TRPV1 mRNA to a DNA fragment. RNA samples from human breast carcinoma cell lines were kindly provided by Dr. Kornélia Polyák (Dana-Farber Cancer Institute, Boston, MA, USA). RNA isolation from ATCC cell lines was performed with TRIzol reagent (Invitrogen, Carlsbad, CA) according to the manufacturer's instructions. Total RNA (600 ng) was reverse-transcribed with RevertAid™ H Minus First Strand cDNA Synthesis Kit (Fermentas). RT-reaction products (5% of the total RT-reaction volume) were used as templates for the PCR: 95 °C denaturing for 30 s, 60 °C annealing for 30 s, and 72 °C extension time for 40 s, using Taq DNA polymerase (Fermentas). The TRPV1 transcripts of prostate and breast carcinoma cell lines was synthesized with specific primer pairs (40 cycles): i) N-TRPV1 forward 5′-ATG AAG AAA TGG AGC AGC ACA GAC-3′ (exon 1) and reverse 5′-CAC CTC CAG CAC CGA GTT CTT CT-3′ (exon7) producing a 1256 bp fragment ii) C1-TRPV1: forward 5′-CTC CTA CAA CAG CCT GTA C-3′ (exon 13) reverse 5′-AAG GCC CAG TGT TGA CAG TG-3′ (exon 16) producing a 679 bp fragment Primer pairs for GAPDH (20 cycles) was used as a positive control: forward 5′-GGT GGT CTC CTC TGA CTT CAA CA-3′ (exon 7) and reverse 5′-GTT GCT GTA GCC AAA TTC GTT GT-3′ (exon 8) producing a 127 bp fragment. The RT-PCR profiling of TRPV1 specific mRNA species, either from human prostate or breast carcinoma cell lines were carried out with three independent total RNA samples. PCR products were size separated on agarose gels and visualized with CyberGreen staining.

2.5. Western blot analysis

The protocol of the Western blot analysis is described in detail elsewhere [33]. Briefly, protein extracts (50 μg) were loaded on 10% SDS polyacrylamide gels. After protein transfer the nitrocellulose membranes were split at the position of proteins of 40 kDa. Antibodies used and their dilutions were: anti-TRPV1 (1:200; rabbit polyclonal, Thermo Scientific, Rockford, IL, #PA1-748) and anti-GAPDH (1:10,000; rabbit polyclonal, Sigma Aldrich, #SAB2100894) and anti-rabbit-HRP (1:10,000; goat secondary, Sigma-Aldrich, #A5420). The specificity of the TRPV1 antibody was verified previously [17]. Optical density (OD) values of the bands on Western blot images were determined with ImageJ software. Average OD values of TRPV1 protein were normalized to those of GAPDH. The TRPV1 protein levels were compared between cancer cell lines and human TG using paired student t-test. Differences were considered significant if the p value was <0.05.

2.6. RTX treatment of rats

Experiments were carried out in 3-months old male Wistar rats. RTX (1 mg) was dissolved in 500 μl ethanol (96%) and diluted in physiological saline and injected subcutaneously into the scruff of the neck in a volume of about 100 μl. The RTX was applied at the dosage of 20 μg/kg body weight daily for three days under light ether anesthesia to avoid unnecessary pain. Control rats received vehicle (saline). Three rats per group were used. Denervation was tested with the CAPS eye wipe-test [33,34]. Briefly, 50 μl CAPS solution (500 μM in PBS) was administered to the rat cornea. The evoked eye-wiping movements were counted. Ten days later animals were sacrificed and prostate samples were collected for immunostaining. Animal experiments were performed in accordance with national (1998th XXVIII.) and European (2010/63/EU) animal ethics guidelines. Experimental protocols were approved by the Review Committee of Biological Research Centre Hungarian Academy of Sciences, then by the

responsible governmental agency (clearance numbers: XVI./03047-1/2008).

2.7. Immunofluorescence staining

Frozen sections were prepared from rat prostate gland as described elsewhere [22]. Specific antibodies were used at dilutions that gave the best signal relative to non-specific staining. The following antibodies were used: anti-TRPV1 (1:1000; rabbit polyclonal, ABR Affinity Bioreagents #PA1-747), and anti-rabbit-TRITC (1:1000; goat secondary, Sigma-Aldrich, #T6778). The specificity of the TRPV1 antibody was verified previously [17]. The specimens were mounted with fluorescent mounting medium (Dako) and viewed with a Nikon Eclipse E600 microscope equipped with epifluorescence and photographed with a Spot RT Slider camera. The images were processed using SPOT software (version 4.0.9 for Windows; Diagnostic Instruments).

2.8. Vanilloid-induced Ca²⁺ transport

Radioactive $^{45}Ca^{2+}$ uptake was assayed in prostate and breast cancer cells as was described previously [33]. Briefly, cells were plated in 96 well plates at approximately 50% confluence. The next day $^{45}Ca^{2+}$ uptake was performed for 10 min in assay medium (Ca²⁺- and Mg²⁺-free Hanks Balanced Salt Solution supplemented with 0.8 mM MgCl₂, 25 mM TRIS-HCl and with 0.1 μCi/ml of $^{45}Ca^{2+}$ as radioactive tracer, pH = 7.4). The assay medium was used with or without 2 μM CAPS. As positive controls $^{45}Ca^{2+}$ uptake was carried out in isolated rat DRG cultures and in cancer cell lines ectopically expressing TRPV1 receptor. The same treatment was applied for 3–4 parallel wells and the average counts per minute values were calculated. Paired Student t-test was used to evaluate the difference. A p value <0.05 was considered as statistically significant. In another experiment, the effect of thapsigargin (3 μM) or ionomycin (3 μM) was tested resulting in a dose-response curve for CAPS using the stably transfected HaCaT^{TRPV1} cell line. Thapsigargin and ionomycin was added to the assay medium containing a serial dilution of CAPS. The same treatment was applied for three parallel wells and the average counts per minute values were calculated. Dose-response curves were plotted to the average counts per minute values and EC₅₀ values were calculated. Dose-response curves were compared with an extra sum of squares F-test using Prism3 (GraphPad Software, Inc., San Diego, CA) software.

2.9. Cell viability assay

Cells were seeded at 30,000 cells/well in 96-well plates 24 h before adding RTX/CAPS/menthol-containing solutions, all samples in quadruplicates (four parallel wells), then plates were further incubated for 24 h at 37 °C. Cell survival was determined by the colorimetric XTT assay according to the instructions of the manufacturer (Sigma). Absorbance of converted dye was measured at a wavelength of 450 nm. The values from quadruplicates were averaged and compared to the average value of the non-treated control (100% viability). Student t-test was applied to analyze differences. Differences were considered significant if the p value was <0.05.

2.10. Monitoring cell division and activity of caspase-3

MCF7 cells were transiently transfected with pGFP-TRPV1 with Mirus transfection reagent. The next day approximately 10,000 cells/well were seeded in 96-well plates in DMEM medium and grown for 3 days. Cells were monitored using the Live Cell Imaging System (Incucyte, EssenBioScience, Michigan, USA) by acquiring images every 1 h. Three 780 μm ∗ 625 μm region per well were examined. In order to monitor the caspase-3 activity, cells were transfected with pmAmetrine-DEVD-tdTomato (Addgene #18879) together either with pTRPV1 or with pLuciferase (as negative control) using Mirus transfection reagent.

Appearance of green fluorescence correlates with specific activation of caspase-3 [35].

2.11. Ca^{2+} imaging

Cells grown on collagen-coated glass bottom 35 mm dishes (MatTek Corp., Ashland, MA) were loaded with the cell permeable acetoxymethyl (AM)-ester form of the indicator dyes. The following dyes were used: for cytoplasmic free Ca^{2+} concentration (c_{cyt}): Fluo-4-AM (1 μM) and for mitochondrial free Ca^{2+} concentration (c_{mito}) Rhod-2-AM (1 μM) (Invitrogen) were diluted in cell culture media for 20 min at room temperature. Cells were loaded with 1 μg/ml CellMask™ Orange Plasma membrane Stain (Life Technologies) for 20 min in the culture media in some experiments. After loading cells were washed with buffer solution (DPBS) used for Ca^{2+}-imaging experiments contained (in mM): NaCl 138, Na_2PO_4 8, $CaCl_2$ 2, $MgCl_2$ 0.5, KCl 2.7, KH_2PO_4 1.6; pH 7.4. In Na^+-free solutions, NaCl and Na_2HPO_4 were replaced with equimolar N-methyl-D-glucamine. In Ca^{2+}-free solution, $CaCl_2$ was replaced with 10 mM EGTA. In some experiments, propidium iodide (2 μM final concentration) was added to the buffer solution. We used an inverted confocal microscope DMI6000 integrated to a Leica TCS-SP5 workstation to examine changes of c_{cyt} or c_{mito}. The 488-nm excitation wavelength was used to illuminate Fluo-4 and GFP-TRPV1. The 561-nm laser was used for Rhod-2, CellMask™ Orange and propidium iodide. At the confocal microscope, fluorescence emission was recorded at 510–554 nm (Fluo-4, GFP-TRPV1) and 584 to 683 nm (Rhod-2, CellMask™ Orange, propidium iodide). Recordings were performed at 37 °C using Tempcontrol 37-2 digital, and a Heating Stage, all from PeCon GmbH

(Erbach, Germany). The drugs were added to the abovementioned solutions by pipette and remained in the solution until the end of the experiments. In some experiments differential interference contrast images were also collected to assess morphological changes of cells. In other experiments fluorescence images for either c_{cyt} or c_{mito} measurements were collected simultaneously. Circular-shaped regions of interest (ROI) were placed inside the cytoplasmic area of cells. The fluorescence values were calculated after background subtraction (fluorescence intensity of regions without cells). Fluorescence intensity values were normalized in each experiment to the averaged basal value measured during the non-treated period. Bleaching correction was carried out, when the baseline was not stable. The LAS-AF (Leica, Wetzlar, Germany), ImageJ and Prism3 software were used for data analysis.

3. Results

3.1. Expression patterns of TRPV1 in cancer cell lines and human TG

We focused on the TRPV1 expression profile in human prostate glands (at the cellular level) of healthy and prostate cancer patients using a miniaturized RT-PCR protocol using LCM-dissected microscopic specimens. To determine TRPV1 expression at high spatial resolution, 10–20 human epithelial gland cells and stroma cells were dissected by LCM followed by a miniaturized RNA isolation required for RT-PCR. Expression of TRPV1 was only evident in the prostate gland epithelium, while stroma cells were negative (Fig. 1A). Next, we focused on the epithelial layers of normal and neoplastic cell populations by choosing morphological markers with the help of the LCM microscope. Cell
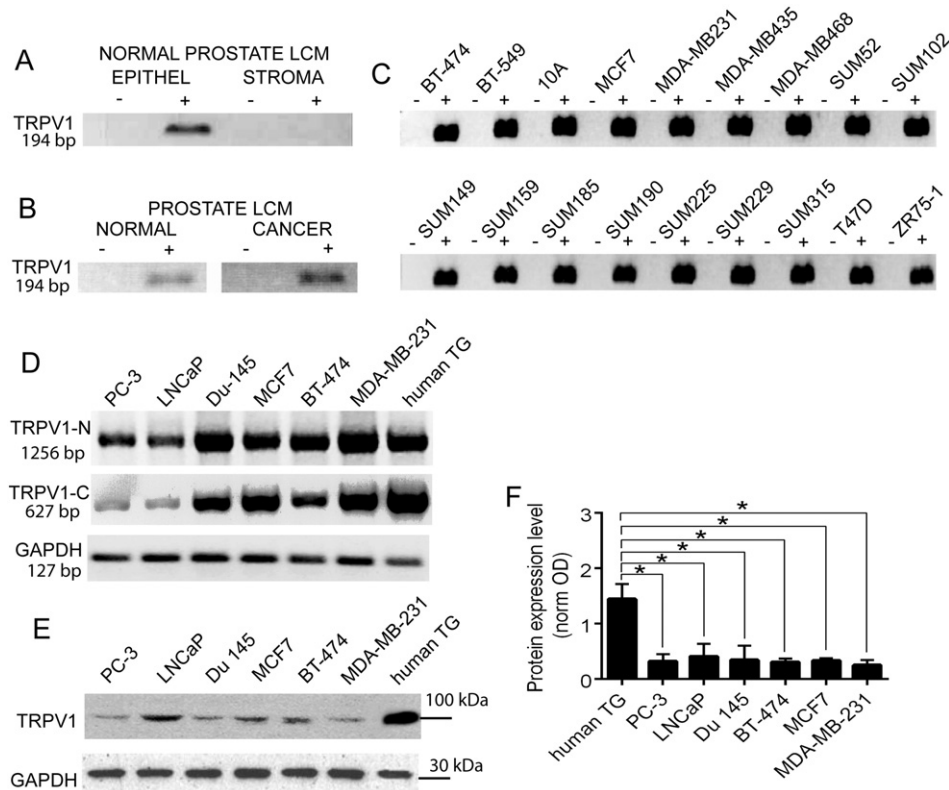

Fig. 1. Detection of TRP channel isoform transcripts in cell lines and tissue by RT-PCR and Western blot. A) LCM technology allowed to dissecting epithelial layers from stroma, in both normal and tumor tissue from prostate. TRPV1 expression was restricted to epithelial cells and absent in the stroma. In samples marked with (−) in panels B–D, no RT enzyme was added. The results were identical in three independent tissue samples and one is shown. B) Epithelial cells with normal or neoplastic morphology expressed TRPV1 mRNA expression in the prostate tissue. C) All breast cancer cell lines (18 out of 18) expressed TRPV1 mRNA evidenced by the 194-bp RT-PCR fragment. D) Signals for the different TRPV1 transcript using two different primer pairs were found in cell lines derived from prostate cancer-derived (lanes 1–3) and breast cancer-derived (lanes 4–6) cell lines, as well as from human TG tissue (line 7). The normalization with the GAPDH housekeeping control allowed to qualitatively assessing the abundance of the different transcripts present in each sample. E) On Western blots, a strong positive signal (97 kDa) for TRPV1 protein expression was seen in TG and in BT-474 cells; weak signals were also detected in the other 5 cell lines. GAPDH protein was used as control. F) Quantification of average OD values for TRPV1 normalized to those of GAPDH are shown. Each column bar is from three independent determinations and represents mean + standard deviation. Significant differences between samples from human TG and cancer cells are marked with * ($p < 0.05$).

samples were captured from freshly dissected prostate tissues obtained from patient biopsies. The TRPV1 transcript was present in prostate cancer-affected foci, both in the tumor tissue as well as in the adjacent untransformed part of the gland, traced by the cellular resolution of LCM (Fig. 1B). In the absence of RT enzyme, no amplification of a TRPV1 fragment was detected in all samples, indicating that the amplicons were indeed resulting from the TRPV1-specific mRNA. To verify the epithelial origin of expression of TRPV1 also in breast tumors, total RNA was prepared from 18 breast carcinoma cell lines. As in prostate carcinomas and derived cell lines, 18 out of 18 breast carcinoma cell lines showed robust expression of TRPV1 (Fig. 1C). Prostate and breast carcinoma cell lines (three of each type) were tested for the presence of thermosensitive TRP channel transcripts (Fig. 1D). A signal for TRPV1 mRNA was present in all six cell lines; semi-quantitative RT-PCR analyses, i.e. a cycle number for PCR reactions not reaching the plateau phase allowed for an estimation of transcript levels. In the case of the N-TRPV1 primer pair, the gel showed a nearly equally strong signal for each sample with a slightly weaker one in PC-3 and LNCaP cells. This indicated that the PCR reaction probably reached the plateau phase or that TRPV1 transcripts were present in cancer cell lines in amounts similar to the one determined in human TG (Fig. 1D, upper row). In the case of C-TRPV1 primer pairs, the gel showed different band intensities. The strongest signal was observed in the sample from human TG (Fig. 1D, middle row). GAPDH was used as internal control (Fig. 1D, lower row). At the protein level, Western blot analysis revealed that all cell lines expressed lower levels of TRPV1 compared to TG (Fig. 1E). Densitometric analysis revealed that human TG expressed significantly higher levels of TRPV1 protein than either breast or prostate cancer cells. Approximately 7–8 fold more TRPV1 protein was detected in the sample from human TG (Fig. 1F). If taking into account that human TG samples contain not only cell bodies of TRPV1-positive pain-sensing neurons, but also TRPV1-negative proprioceptive neurons and satellite cells, then the differences in TRPV1 expression levels per cell between TRPV1-positive sensory neurons and cancer cells is likely even higher.
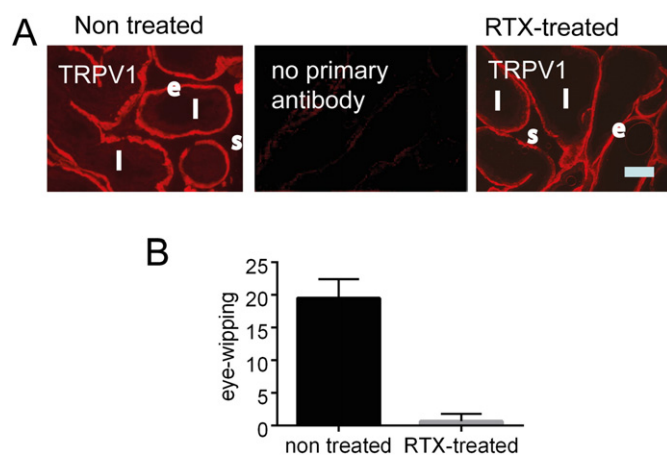
3.2. Testing the effect of RTX treatment on expression levels of TRPV1 in prostate gland tissue

Immunohistochemistry revealed the cellular localization of TRPV1 in rat prostate gland tissue. Immunofluorescence signals for TRPV1 were restricted to the epithelial cell layer (Fig. 2A, left image) confirming the LCM results, where TRPV1 mRNA was detected in epithelial, but not in stromal cells. When the primary antibody was omitted, no fluorescence signal was observed on the prostate tissue sections, further demonstrating the specificity of the TRPV1 antibody (Fig. 2A, middle image). Systemic RTX administration (20 μg/kg body weight daily for 3 days), which was previously demonstrated to eliminating all TRPV1-expressing sensory neurons, did not affect the expression pattern of TRPV1 in the prostate epithelium (Fig. 2A, right image). Thus, our findings indicate that prostate gland epithelial cells, like human keratinocytes [13,36] are resistant to systemic vanilloid treatment in vivo despite the presence of TRPV1 in these cells. As a positive test to validate RTX treatment efficiency, the ablation of TRPV1-positive sensory neurons was confirmed by the capsaicin eye-wipe test (Fig. 2B). The loss of corneal sensitivity to CAPS is a result of the loss of sensory neurons caused by RTX treatment [17].

3.3. Different TRPV1-mediated responses in cancer cells compared to sensory neurons

TRPV1-mediated cytotoxicity is associated with Ca^{2+} accumulation in the mitochondria [23,24] and excessive Na^+ influx across the plasma membrane [22]. Thus, intracellular Ca^{2+} accumulation was measured by a $^{45}Ca^{2+}$ uptake assay in the 6 cell lines and in rat DRG neurons. In CAPS-treated rat DRG neurons a significant increase in Ca^{2+} accumulation occurred when compared to Ca^{2+} accumulation in control neurons (Fig. 3A). In all tumor cell lines CAPS had no measurable effect on mitochondrial Ca^{2+} accumulation, i.e. no differences were observed in comparison to untreated cells (Fig. 3A). This hinted that endogenous TRPV1 expression levels were too low to result in measurable Ca^{2+} uptake or that they were not functional in cancer cells. In order to ascertain mitochondrial and not endoplasmic reticulum Ca^{2+} uptake in this assay, HaCaT^{TRPV1} cells were treated with thapsigargin (3 μM), a specific blocker of sarcoendoplasmic reticulum calcium transport ATPase (SERCA). Mitochondrial Ca^{2+} accumulation measured at different CAPS concentrations was not altered in the presence of thapsigargin indicative of mitochondria-specific Ca^{2+} uptake (Fig. 3B). The EC_{50} values for CAPS were virtually the same; 66 versus 73 nM. The difference between the two dose-response curves was not significant (extra sum of squares F-test, $p > 0.05$). On the other hand, treatment of cells with ionomycin, an ionophore forming pores for Ca^{2+} ions in all cellular membranes, completely abolished the mitochondrial Ca^{2+} accumulation (Fig. 3B). Next, we directly monitored the free mitochondrial matrix Ca^{2+} concentration (c_{mito}) by using the Ca^{2+} indicator dye Rhod-2. Approximately 50% of sensory neurons responded to CAPS (20 μM) with an immediate rise in c_{mito} (Fig. 3C), as well as in c_{cyt} (Fig. 3D). However, such an increase in c_{mito} wasn't observed in all 6 carcinoma cell lines, even at a higher CAPS concentration (50 μM; Fig. 3E–J). In few PC-3, MCF7 and Du 145 cells, small brief Ca^{2+} transients in c_{mito} were detected upon CAPS administration, exemplified by recordings of single cells (red traces in Fig. 3E–J). The ionomycin-evoked increase in c_{mito} was used as positive control to show the proper loading of the Ca^{2+} indicator Rhod-2 (Fig. 3E–J). The application of CAPS (20 μM) to rat DRG neurons led to cell swelling, axonal retraction and fragmentation (Fig. 3K). In some cases the cell swelling was so pronounced that it resulted in membrane disruption and necrotic cell death, as was shown before [22]. CAPS-treated carcinoma cells neither showed cell swelling nor membrane bleb formation. No obvious morphological changes were observed in all cancer cell lines except in MCF7 cells. In these cells treated with 50 μM CAPS formation of
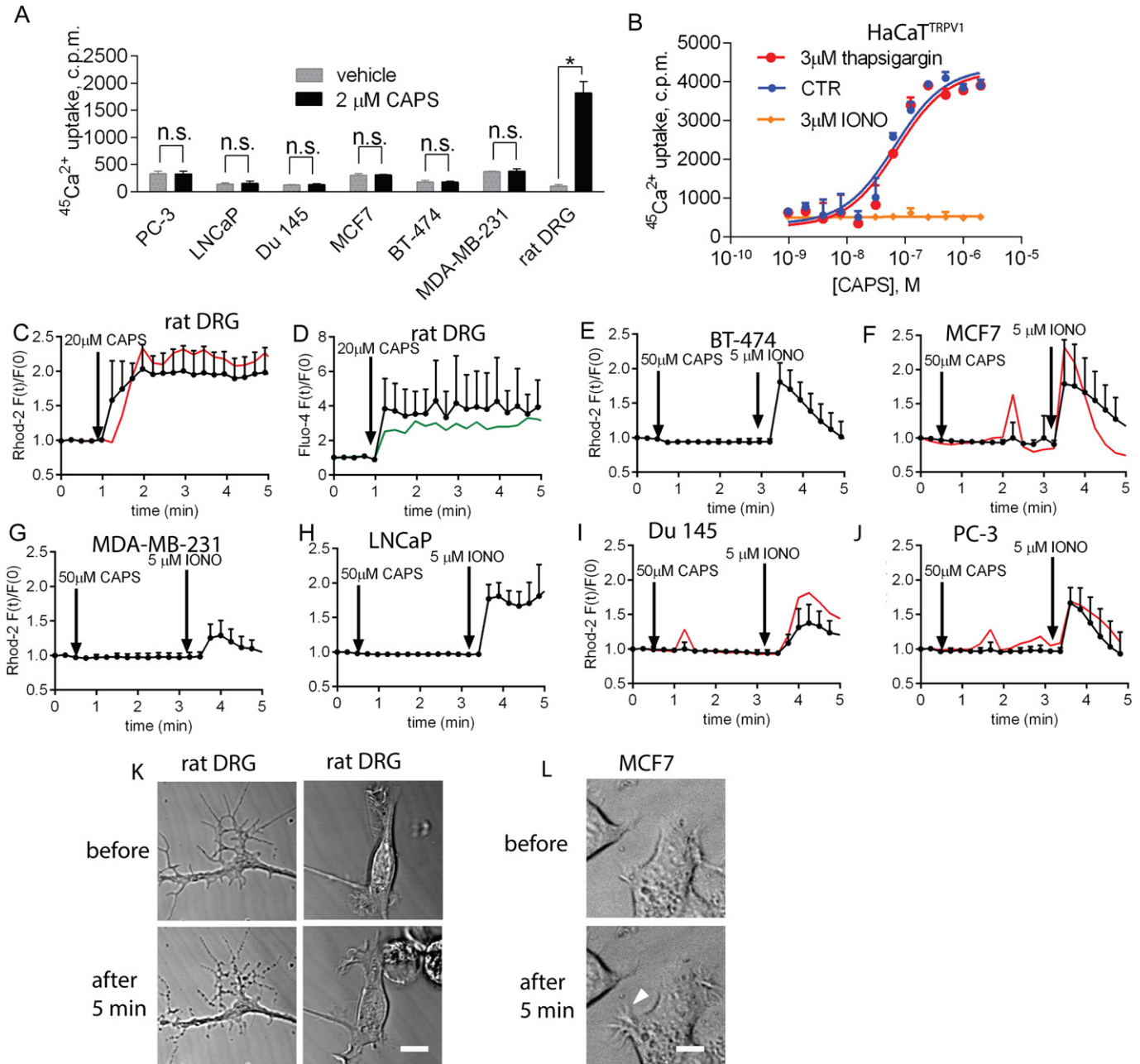

Fig. 2. Immunofluorescence staining for TRPV1 on rat prostate gland sections. A) Rats were either denervated with subcutaneous RTX administration or treated with saline (control group). Sections were stained with a TRPV1-specific antibody. No significant changes in immunofluorescence intensity were observed in the epithelia after denervation. The abbreviations represent luminal (l), epithelial (e) and stromal (s) part of the prostate gland. Scale bar represents 0.5 mm. Similar images were obtained from all animals (control, non-treated (left); RTX-treated (right)). No signal was observed when the primary antibody was omitted (middle). B) The capsaicin eye-wipe test demonstrated the effective ablation of TRPV1-positive neurons after RTX treatment.

Fig. 3. TRPV1-mediated Ca^{2+} accumulation. A) Insignificant TRPV1-mediated Ca^{2+} uptake evoked by CAPS (2 μM) treatment (black bars) in all cancer cell lines in comparison to non-treated cells (gray bars). Similar treatment of rat DRG neurons resulted in a clear Ca^{2+} uptake. Bars represent the mean of $^{45}Ca^{2+}$ counts per minute (c.p.m.) + standard deviation (S.D.) values that were calculated from four parallel wells. Experiments were repeated three times with similar results. B) While thapsigargin had no effect on the [CAPS]-dependent $^{45}Ca^{2+}$ uptake in TRPV1/MCF7 cells (compare red and blue curves), ionomycin abolished specific uptake (orange line). Dots represent mean + S.D. values from four parallel wells. Experiments were repeated three times with similar results. C–D) Application of CAPS (20 μM) resulted in a rapid increase in c_{mito} (C) and in c_{cyt} (D) in approximately 50% of DRG neurons. Black dots represent average c_{mito} (C) and c_{cyt} (D) calculated from 10 cells + standard deviation. Red (C) and green (D) lines represent single recordings. E–J) Measurements of c_{mito} with Rhod-2 in cancer cell lines. Application of CAPS (50 μM) had no effect in most cancer cells. Black dots represent average c_{mito} calculated from 10 cells + standard deviation. Few MCF7 (F), Du 145 (I) and PC-3 (J) cells showed transients in c_{mito} (red lines — single cell recordings). An increase in c_{mito} was induced by ionomycin in all cells (5 μM). K, L) Structural changes after CAPS treatment in DRG neurons and MCF7 cells. The arrow in L) points to pseudopodia formation in CAPS-treated MCF7 cells. Scale bar represents 10 μm.

pseudopodia, cell membrane protrusions involved in tumor cell migration, were observed (Fig. 3L).

3.4. Testing the vanilloid-sensitivity of breast and prostate carcinoma cells in vitro

The cytotoxic potencies of CAPS and RTX to induce cell death was determined in an XTT survival assay carried out in prostate (Fig. 4B,D) and breast cancer cell lines (Fig. 4A,C). As hypothesized and in line with results from previous studies, all cell lines were sensitive to CAPS

(Fig. 4A,B), however only at rather high concentrations (>100 μM) in comparison to concentrations leading to overstimulation toxicity in peripheral nerve cells [22]. The dose/response curves for CAPS and RTX were very similar for all cell lines, irrespective of their origin (breast or prostate). The CAPS structural analog, but ultra-potent TRPV1 agonist RTX was more effective in decreasing the cell viability than CAPS: the half-maximal effect of CAPS was at approximately 200–300 μM vs. the half-maximal effect of RTX at 10 μM in prostate cancer cells (Fig. 4B,D). Interestingly, a small, but generally significant increase of cell viability was observed in a concentration range of CAPS around
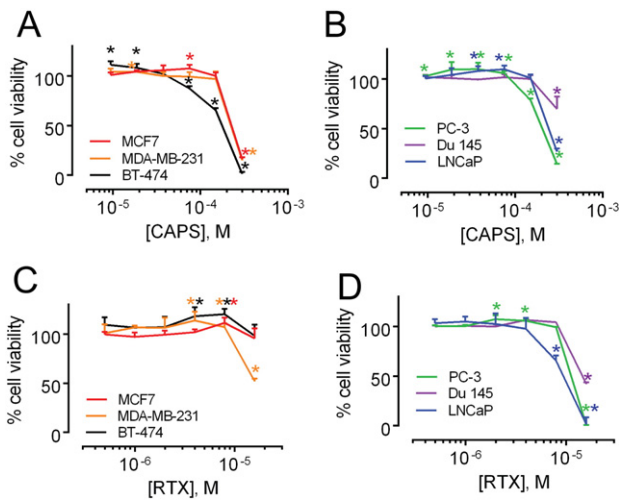
Fig. 4. Vanilloid sensitivity of individual breast cancer (A, C) and prostate cancer (B, D) cell lines. Neither CAPS (A and B) nor RTX (C and D) were effective to reduce the cell viability at low concentrations determined by XTT assays. At low micromolar concentrations, agonists slightly, but in some cases significantly increased the cell viability. At high doses (>100 μM CAPS, >15 μM RTX) viability was decreased in most cell lines. The concentration of 15 μM RTX is way above the concentration necessary to ablate DRG neurons. Each point represents the mean + standard deviation from four parallel wells and experiments were repeated two times with similar results. Significant differences between treated and non-treated cells (100% viability) are marked with * ($p < 0.05$).

10 μM (Fig. 4A,B), where Ca^{2+} oscillations in c_{cyt} were observed (L. Pecze et al., Ms. in preparation).

3.5. Ectopic expression of TRPV1 sensitize cancer cells to TRPV1 agonists

Although all 6 cancer cell lines expressed TRPV1 protein (Fig. 1E), application of CAPS (50 μM) neither resulted in mitochondrial Ca^{2+} accumulation (evidenced by essentially unaltered c_{mito}) nor led to cytotoxicity. With the aim to render these cells more susceptible to TRPV1-mediated cytotoxicity, all cell lines were transiently transfected with a cDNA coding for human full-length TRPV1 and experiments were carried out 24–48 h post-transfection. In all transfected cell lines exposed to a much lower concentration of CAPS (2 μM), significant Ca^{2+} accumulation was observed when compared to TRPV1-transfected cells treated with vehicle (DMSO, final concentration 0.1%) (Fig. 5A). Treatment of MCF7^{TRPV1} cells with even lower CAPS (50 nM) caused an increase in c_{cyt} and c_{mito} displaying various kinetics (Fig. 5B). The increases in c_{mito} were always slightly delayed compared to increases in c_{cyt}, i.e. c_{cyt} values had to reach a certain threshold in order to lead to mitochondrial Ca^{2+} accumulation (Fig. 5B). To better estimate relative TRPV1 levels and to correlate TRPV1 levels with the kinetics and magnitude of responses in c_{cyt} and c_{mito} MCF7 cells ectopically expressing GFP-tagged TRPV1 (MCF7$^{GFP-TRPV1}$) were generated. Application of CAPS (50 nM) resulted in elevations in c_{mito}, while non-transfected MCF7 cells were refractory to CAPS administration (Fig. 5C). Plotting the mitochondrial response to CAPS administration against the GFP fluorescence intensity indirectly reflecting the level of TRPV1 expression revealed a threshold value, i.e. TRPV1 had to reach a certain expression level to allow for mitochondrial Ca^{2+} accumulation (Fig. 5D). Although mitochondrial Ca^{2+} accumulation triggers apoptotic cell death [37], recently it was found that TRPV1 activation induces necrotic and not apoptotic cell death in MCF7 cells over-expressing TRPV1 [38]. Since necrotic cell death is associated with the loss of membrane integrity, in order to decipher the key steps in the process of necrotic death, we focused on the changes of the plasma membrane structure. After administration of 50 μM CAPS, membrane bleb formation and membrane disorganization was seen in MCF7$^{GFP-TRPV1}$ cells, but no structural changes were observed in the neighboring non-expressing cells (Fig. 5E). Prior to membrane bleb formation, an

immediate strong increase in c_{cyt} was seen. For cell membrane visualization, cells were labeled with the CellMask™ Orange dye and for c_{cyt} monitoring, the Ca^{2+} indicator Fluo-4 was used (Fig. 5F). While shortly after CAPS application, the morphology of MCF7^{TRPV1} cells was unaltered, at later times (8 min) big blebs were formed and moreover the entire cells became swollen. This in turn led to loss of plasma membrane integrity and necrotic cell death, evidenced by nuclear propidium iodide incorporation (Fig. 5G). Bleb formation depended on the presence of extracellular Na^+ and Ca^{2+} ions. No blebs were formed in the absence of extracellular Na^+ ions, even when Ca^{2+} entered the cell immediately after CAPS stimulation (Fig. 5H). Extracellular Ca^{2+} ions were also shown to be essential for bleb formation. In the absence of extracellular Ca^{2+} ions (all extracellular Ca^{2+} ions were chelated by 10 mM EGTA), cells didn't show cell swelling (Fig. 5I). Monitoring the intracellular Ca^{2+} concentrations in cells treated with CAPS in the absence of extracellular Ca^{2+} revealed a short-lasting increase in c_{cyt}, which rapidly recovered to basal levels (Fig. 5J; red trace). The transient rise in c_{cyt} is most probably the consequence of endoplasmic reticulum Ca^{2+} depletion. When CAPS was applied in conditions of complete (black trace) or Na^+-free medium (green trace), the continuous Ca^{2+} influx resulted in permanently elevated c_{cyt} levels. This indicated that TRPV1-mediated Na^+ and Ca^{2+} influxes were responsible for membrane bleb formation and necrotic cells death.

3.6. Ectopic expression of TRPV1 decreases cancer cell survival by induction of apoptosis and necrosis

When MCF7$^{GFP-TRPV1}$ cells obtained after transient transfection were maintained in cell culture for longer periods, at around day 3, cells stopped to grow and did not show mitosis. In contrast, the untransfected non-green MCF7 cells also present in the same petri dishes showed normal proliferation. Transfected MCF7 cells often started to display strong green fluorescence, i.e. GFP-TRPV1 expression immediately after mitosis. This might be linked to the fact that the GFP-TRPV1 construct is driven by the CMV promoter that shows strong cell-cycle dependent activity [39]. The fraction of MCF7$^{GFP-TRPV1}$ cells with a flattened polygonal morphology was likely the cell cycle-arrested ones; none of the strongly green MCF7$^{GFP-TRPV1}$ cells divided within the next 50 h (Fig. 6A). Many of the remaining MCF7$^{GFP-TRPV1}$ cells displayed signs of apoptosis (cell shrinkage, picnotic nuclei) even in absence of exogenous agonist stimulation (yellow, orange and upper red cells in Fig. 6A). In untransfected cells mitosis was observed regularly (blue cells in Fig. 6A). The induction of apoptosis was further investigated in MCF7^{TRPV1} cells; they were co-transfected with the FRET-based caspase-3 indicator pAmetrine-DEVD-dtTomato. During the first 2 days post transfection, approximately 50–60% of the MCF7^{TRPV1} cells showed strong activation of caspase-3 and underwent apoptosis (Fig. 6B, upper row). Since the transfection efficiency was found to be 50–60% in these cells, virtually all co-transfected cells showed the signature of caspase-3 mediated apoptosis. In control experiments, where MCF7 cells were co-transfected with pAmetrine-DEVD-dtTomato and pLuciferase, the percentage of cells undergoing spontaneous apoptosis via activation of caspase-3 was in the order of 3–5% (Fig. 6B, lower row).

4. Discussion

Currently three ways are known how sensory neurons expressing TRPV1 channels respond to exogenous agonists in a concentration-dependent way: low stimulation leads to TRPV1 channel activation, stronger stimuli may cause channel desensitization (temporal inhibition) and finally prolonged and excessive activation leads to overstimulation-based cytotoxicity. Physiological TRPV1 activation e.g. mediated by low doses of CAPS increases the frequency of spontaneous Ca^{2+} oscillations in sensory neurons [40] leading to pain sensation. CAPS and RTX application at higher concentrations are temporally desensitizing [41] and
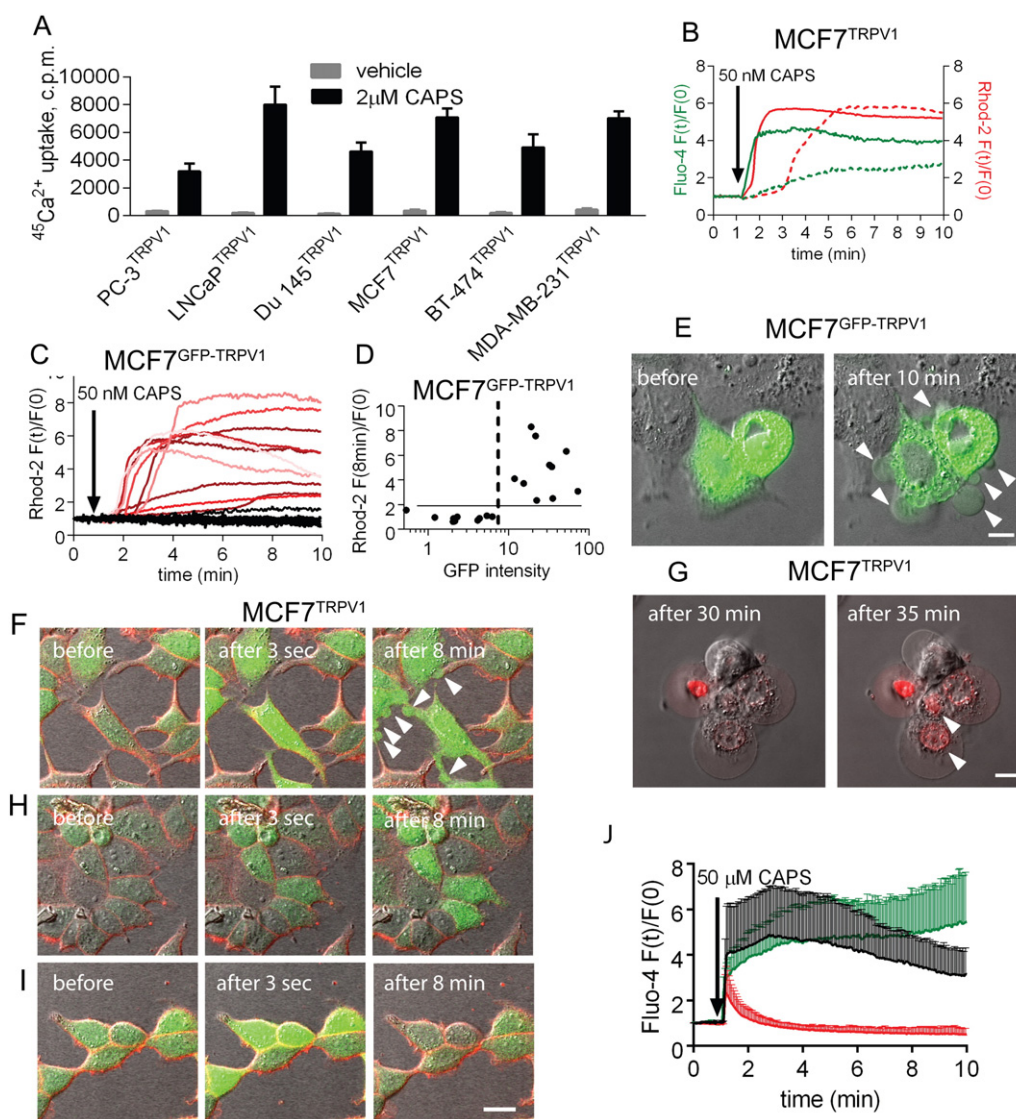
Fig. 5. TRPV1-mediated Ca^{2+} accumulation A) Ectopic expression of TRPV1 resulted in a strong CAPS-induced Ca^{2+} accumulation in all transfected cell lines: compare non-treated cells (gray bars) with CAPS-treated cells (black bars). The increase was on average, ~10–20 fold of base line $^{45}Ca^{2+}$ influx. Experiments were carried out side-by-side, either in the absence (blue and green bars) or in the presence of 2 μM CAPS (red and purple bars) in the uptake medium. Bars represent the mean of $^{45}Ca^{2+}$ counts per minute (c.p.m.) + standard deviation (S.D.) values that were calculated from four parallel wells. B) Simultaneous measurements of c_{cyt} (green) and c_{mito} (red) in MCF7 cells overexpressing TRPV1. Dashed and solid lines are from representative recordings of two cells. C) Increase in c_{mito} in MCF7^{TRPV1} cells after CAPS (50 nM) treatment. For these experiments a GFP-tagged version of TRPV1 was used that allows to indirectly determining TRPV1 concentrations by measuring cellular GFP expression. Mitochondrial free Ca^{2+} concentrations were monitored and cells could be divided in responders (~40% of cells; red traces) and non-responders (black traces) D) Plotting the increase in Rhod-2 fluorescence (mitochondrial response) after 8 min of CAPS stimulation against the GFP signal intensity revealed a threshold value. E) Membrane blebs and membrane disorganization (arrowheads) are observable only in MCF7 cells ectopically expressing GFP-TRPV1 treated with 50 μM CAPS. The scale bar is 10 μm. F) MCF7 cells overexpressing TRPV1 channels were loaded with the Ca^{2+} indicator Fluo-4 (green) and CellMask™ Orange plasma membrane stain (red) and treated with 50 μM CAPS. The scale bar is 25 μm. Immediately after treatment a strong rise in c_{cyt} and membrane blebs were observed (arrowheads). G) 30–35 min after CAPS application MCF7^{TRPV1} cells showed strong cell swelling and membrane blebbing leading to loss of membrane integrity, also evidenced by nuclear propidium iodide incorporation (arrowheads). H–I) In the absence of either extracellular Na^+ (H) or Ca^{2+} ions (I) no blebs were formed. J) The time-lapse recordings show changes in c_{cyt} upon CAPS stimulation in complete (black curve) Na^+-free (green curve) and Ca^{2+}-free (red curve) cell culture medium. Bars represent the mean of the relative fluorescence intensity values + standard deviation.

systemic or topic RTX application at ablative doses for pain-sensing neurons result in pain relief [17].

In our study we investigated the TRP-mediated overstimulation toxicity in TRPV1-expressing prostate and breast cancer cells. In pain-sensing neurons of the peripheral nerve system, the mechanisms of TRPV1 agonist-induced cell toxicity have been elucidated in some detail. Initially robust Na^+ and Ca^{2+} influx across the plasma membrane is occurring. The intracellular Na^+ accumulation is responsible for the cell swelling and the cause for rapid necrotic-like cell death [22]; Ca^{2+} uptake is responsible for the mitochondrial Ca^{2+} accumulation [23] leading to apoptosis. In none of the investigated cancer cell lines we found evidence for either mitochondrial Ca^{2+} accumulation or cell swelling upon stimulation with CAPS at concentrations ≤50 μM, a concentration below the one resulting in non-TRPV1-mediated, non-specific effects. Based on our results we concluded that TRPV1 expression levels are a key factor for TRPV1-mediated cytotoxicity. Nonetheless also the agonists' potency to activate TRPV1 (RTX > CAPS) and the agonist concentration are of importance. Our data suggest that the vanilloid resistance of the cancer cells is the result from too low expression levels of endogenous TRPV1. In support of this idea, overexpression of human TRPV1 in all investigated cancer cells led to cell swelling and membrane blebs in TRPV1-overexpressing cancer cells. Moreover, we observed a threshold phenomenon, where a certain level of TRPV1 (evidenced by the green fluorescence intensity proportional to the
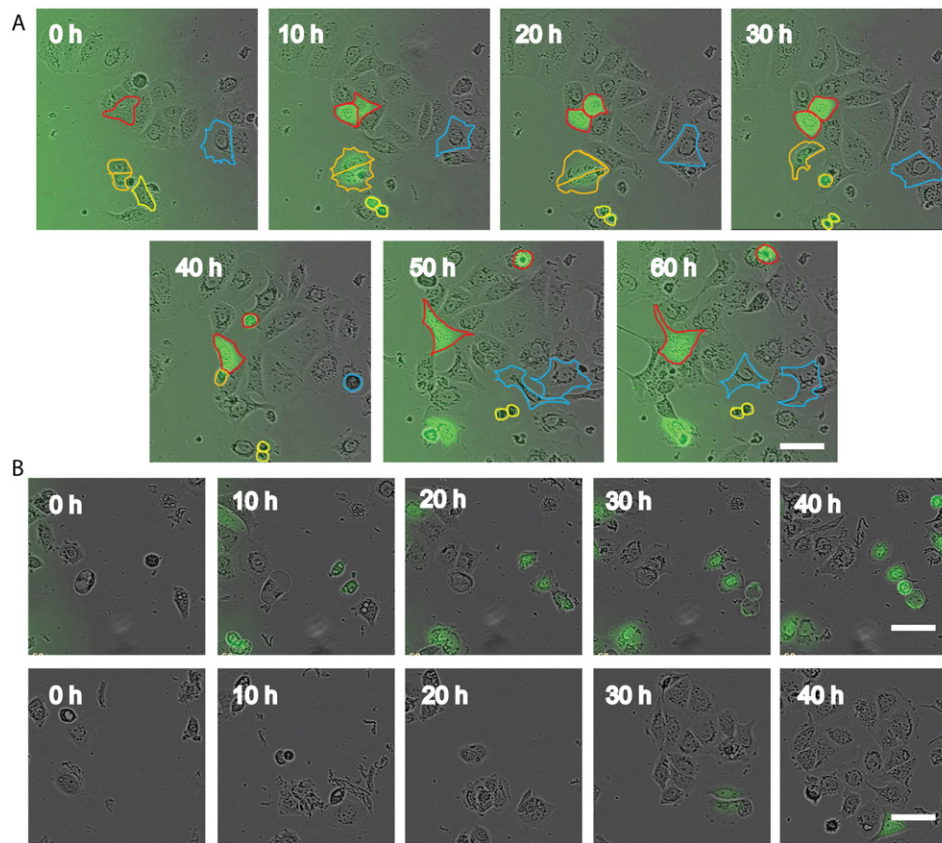
Fig. 6. TRPV1-mediated cell-division arrest in MCF7 ectopically expressing TRPV1 channels. A) MCF7[GFP-TRPV1] cells were monitored and only cells without GFP-TRPV1 expression show mitosis and cell division (cells marked in blue). Cells expressing GFP-TRPV1 showed shrinkage and apoptotic cell death (yellow-, orange- and red-marked cell) or cell cycle arrest (left red-marked cell). The scale bar is 50 μm. B) MCF cells were co-transfected with TRPV1 and the fluorescence-based apoptosis indicator pAmetrine-DEVD-dtTomato (upper row) or a control-plasmid (expressing Luciferase) and pAmetrine-DEVD-dtTomato (lower row). Significantly more apoptotic processes (green fluorescence) were observed in MCF7 cells transiently transfected with TRPV1 channels, approximately 50–60% of cells underwent apoptosis in the period of 40 h following the co-transfection. Spontaneous apoptosis were also observed in control cells, but <5% of cells underwent apoptosis at a given time point.

density of TRPV1 channels) was required to induce massive accumulation of Ca^{2+} in mitochondria (Fig. 5). Thus, the mere presence of TRPV1 protein (evidenced by Western blot analysis) does not automatically signify high sensitivity to vanilloids and moreover the possibility to induce overstimulation cytotoxicity. The vanilloid-insensitivity (to CAPS or RTX) of other TRPV1-expressing cells was also previously shown in keratinocytes [13,36], in lung epithelial cells [42] and in this study, in normal prostate epithelial cells in vivo. Normal prostate epithelial cells were shown to have lower TRPV1 expression levels than cells from prostate cancer patients [30]. Therefore, we assume that the low expression levels of TRPV1 in normal rat prostate epithelial cells are the main cause for the resistance of these cells to RTX treatment in vivo in comparison to the sensitive TRPV1-expressing sensory neurons. Nevertheless, knowing that at the cellular level protein expression levels vary from cell to cell (a stochastic process [43]), we cannot exclude the possibility that in few cells TRPV1 expression levels reached the threshold, where they would become sensitive to RTX treatment. Thus, theoretically a tiny fraction of normal prostate epithelial cells might die resulting from RTX treatment. However, they would be easily replaced by the unaffected neighboring epithelial cells that would fill the gap via cell division. On the other hand, postmitotic sensory RTX-sensitive neurons can't be replaced resulting in the permanent disappearance of TRPV1-positive neurons in samples from sensory ganglia [17]. We observed that the relatively low endogenous TRPV1 expression levels did not result in rapid vanilloid-induced cytotoxicity in breast and prostate carcinoma cell lines at low micromolar concentrations in vitro. CAPS induced cell death at concentrations above 250 μM, at which the cytotoxic effects were presumably not TRPV1-mediated. At millimolar concentration, CAPS (and also RTX) replacing

quinone in the mitochondrial respiratory chain inhibits energy production and induces the generation of an excess of reactive oxygen species that finally leads to apoptotic cell death [44]. Moreover, chemical modification of CAPS by cytochrome P450-dependent monooxygenases to a reactive electrophilic intermediate has been reported [45]. This in turn leads to covalent modification of cellular macromolecules such as DNA, RNA and proteins [46]. Moreover, AMP-dependent protein kinase activation [47], peroxisome proliferation-activated receptor subtype alpha activation [48], p53 phosphorylation [49] and inhibition of nuclear transcription factor-kappa B (NF-κB) [50] are assumed to be involved in TRPV1-independent vanilloid cytotoxicity. These non-specific effects are not unique for cancer cells, because at this concentration, CAPS reduced the growth of all cell types tested in our laboratory including normal human keratinocytes and even insect cells not having a TRPV1 gene ortholog [13]. On the other hand, endogenous TRPV1 channel is functional and its activation led to transient increases in c_{mito} and invadopodium formation in MCF7 cells (Fig. 3L). Thus, TRPV1-specific effects are likely to overlap with TRPV1-independent effects, if cancer cells are exposed to CAPS in the high micromolar range. As an example, generation of reactive oxygen species were shown to be the consequence of TRPV1-mediated [51,52] and TRPV1-independent processes [44].

Interestingly, in cancer cells merely the overexpression of TRPV1 channels decrease the viability of cancer cells. Here we found that mainly apoptotic processes are activated, but mitotic arrest in MCF7[GFP-TRPV1] cells are also observable. The absence of mitosis in the surviving MCF7[GFP-TRPV1] cells subsequently didn't allow for the establishment of permanent MCF7[GFP-TRPV1] clones. Whether this growth arrest phenotype is restricted to cancer cells remains to be

further investigated, since we had been successful to establish cell clones permanently expressing ectopic TRPV1 protein using non-tumor derived cell lines such as HaCaT (spontaneously immortalized keratinocyte cell line from adult human skin) [13] or NIH-3T3 (spontaneously immortalized mouse embryo fibroblast cell line) [53].

Of interest, a case report described that a prostate cancer patient who ingested chili sauce twice a week maintained a stable prostate specific antigen (PSA) reading for a year [54]. PSA is an established marker for the presence and activity of prostate tumors. An oral dose of CAPS (5 mg/kg/day) significantly slowed the growth of PC-3 prostate cancer xenografts in in vivo mouse models [55,56]. The applied dose is expected to result in a systemic CAPS concentration of maximum 16 μM in the tumor environment, i.e. a concentration that has no evident anti-proliferative effect on cancer cells in vitro. On the contrary, the slight but sometimes significant increase in the cell viability and the pseudopodia formation in MCF7 cells subjected to low CAPS concentrations observed in vitro hints that mild activation of TRPV1 channels might rather promote tumor growth in vivo. Further investigations are required to solve the apparent discrepancies between the in vitro and in vivo results.

Tumors are heterogeneous entities, whose growth is dependent on mutual cooperation between genetically altered cancer cells and the surrounding stromal cells, including immune cells, i.e. fibroblasts/myo-fibroblasts (carcinoma-associated fibroblasts), mesenchymal-like cells, vascular smooth muscle cells and endothelial cells [57]. Tumors are also innervated: sympathetic, parasympathetic and sensory [58], i.e. pain sensing TRPV1-positive neurons are also present in certain tumor masses. Pain-sensing neurons have a dual role: I) they detect signals from damaged tissue such as arachidonic acid derivatives and oxidized linoleic acid metabolites (endogenous TRPV1 agonists) present in the tumor milieu [59,60] and II) pain-sensing neurons locally release inflammatory mediators including substance P, Calcitonin Gene-Related Peptide, neurokinin A, endothelin-3 (ET-3), neurosteroids, and others that probably promote tumor growth [61]. Malignant tumors often develop at sites of chronic injury. Tissue injury is considered to have an important role in the pathogenesis of malignant disease, with chronic inflammation being the most important risk factor. Few studies postulate a mutual cooperation between cancer cells and sensory neurons, however this is still a poorly investigated area [62].

Based on our findings that sensory neurons are clearly more sensitive to TRPV1 agonists than prostate and prostate cancer cells, we hypothesize that CAPS or RTX might influence the function of sensory neurons innervating the tumor mass by disturbing the cooperation between cancer cells and sensory neurons. Thus, the effect of vanilloids (desensitization, cytotoxicity) on sensory neurons in the tumor microenvironment might indirectly diminish tumor growth. This might explain in part the difference exerted by CAPS and RTX in vitro and in vivo. In conclusion, additional, likely in vivo experiments are required to investigate the putatively beneficial effects of vanilloids to reduce/prevent tumor growth.

Conflicts of interest

The authors declare that they have no conflicts of interest with the contents of this article.

Authors' contributions

LP designed the study, performed Ca^{2+} measurements, data analysis and wrote the manuscript KJ performed RT-PCR, cloning and Western blot WB performed apoptosis assays PG performed LCM, VC performed XTT analysis and secured funding, ZO wrote the manuscript and performed RT-PCR and secured funding BS performed data analyses and wrote the manuscript and secured funding.

Transparency document

The Transparency document associated with this article can be found, in online version.

Acknowledgements

References

[1] A.E. Dubin, A. Patapoutian, Nociceptors: the sensors of the pain pathway, J. Clin. Invest. 120 (2010) 3760–3772.

[2] Y. Lee, C.H. Lee, U. Oh, Painful channels in sensory neurons, Mol. Cell 20 (2005) 315–324.

[3] M.J. Caterina, M.A. Schumacher, M. Tominaga, T.A. Rosen, J.D. Levine, D. Julius, The capsaicin receptor: a heat-activated ion channel in the pain pathway, Nature 389 (1997) 816–824.

[4] A. Dhaka, V. Uzzell, A.E. Dubin, J. Mathur, M. Petrus, M. Bandell, A. Patapoutian, TRPV1 is activated by both acidic and basic pH, J. Neurosci. 29 (2009) 153–158.

[5] M.J. Caterina, T.A. Rosen, M. Tominaga, A.J. Brake, D. Julius, A capsaicin-receptor homologue with a high threshold for noxious heat, Nature 398 (1999) 436–441.

[6] K. Mitchell, E.E. Lebovitz, J.M. Keller, A.J. Mannes, M.I. Nemenov, M.J. Iadarola, Nociception and inflammatory hyperalgesia evaluated in rodents using infrared laser stimulation after Trpv1 gene knockout or resiniferatoxin lesion, Pain 155 (2014) 733–745.

[7] B. Veronesi, M. Oortgiesen, The TRPV1 receptor: target of toxicants and therapeutics, Toxicol. Sci. 89 (2006) 1–3.

[8] M.H. Vos, T.R. Neelands, H.A. McDonald, W. Choi, P.E. Kroeger, P.S. Puttfarcken, C.R. Faltynek, R.B. Moreland, P. Han, TRPV1b overexpression negatively regulates TRPV1 responsiveness to capsaicin, heat and low pH in HEK293 cells, J. Neurochem. 99 (2006) 1088–1102.

[9] M.J. Gunthorpe, A. Szallasi, Peripheral TRPV1 receptors as targets for drug development: new molecules and mechanisms, Curr. Pharm. Des. 14 (2008) 32–41.

[10] C.E. Deering-Rice, M.E. Johansen, J.K. Roberts, K.C. Thomas, E.G. Romero, J. Lee, G.S. Yost, J.M. Veranth, C.A. Reilly, Transient receptor potential vanilloid-1 (TRPV1) is a mediator of lung toxicity for coal fly ash particulate material, Mol. Pharmacol. 81 (2012) 411–419.

[11] M.G. Sanchez, A.M. Sanchez, B. Collado, S. Malagarie-Cazenave, N. Olea, M.J. Carmena, J.C. Prieto, I.I. Diaz-Laviada, Expression of the transient receptor potential vanilloid 1 (TRPV1) in LNCaP and PC-3 prostate cancer cells and in human prostate tissue, Eur. J. Pharmacol. 515 (2005) 20–27.

[12] P.R. de Jong, N. Takahashi, A.R. Harris, J. Lee, S. Bertin, J. Jeffries, M. Jung, J. Duong, A.I. Triano, J. Lee, Y. Niv, D.S. Herdman, K. Taniguchi, C.W. Kim, H. Dong, L. Eckmann, S.M. Stanford, N. Bottini, M. Corr, E. Raz, Ion channel TRPV1-dependent activation of PTP1B suppresses EGFR-associated intestinal tumorigenesis, J. Clin. Invest. 124 (2014) 3793–3806.

[13] L. Pecze, K. Szabo, M. Szell, K. Josvay, K. Kaszas, E. Kusz, T. Letoha, J. Prorok, I. Koncz, A. Toth, I. Kemeny, C. Vizler, Z. Olah, Human keratinocytes are vanilloid resistant, PLoS One 3 (2008) e3419.

[14] P. Facer, M.A. Casula, G.D. Smith, C.D. Benham, I.P. Chessell, C. Bountra, M. Sinisi, R. Birch, P. Anand, Differential expression of the capsaicin receptor TRPV1 and related novel receptors TRPV3, TRPV4 and TRPM8 in normal human tissues and changes in traumatic and diabetic neuropathy, BMC Neurol. 7 (2007) 11.

[15] L.A. Birder, Y. Nakamura, S. Kiss, M.L. Nealen, S. Barrick, A.J. Kanai, E. Wang, G. Ruiz, W.C. De Groat, G. Apodaca, S. Watkins, M.J. Caterina, Altered urinary bladder function in mice lacking the vanilloid receptor TRPV1, Nat. Neurosci. 5 (2002) 856–860.

[16] S.K. Mishra, S.M. Tisel, P. Orestes, S.K. Bhangoo, M.A. Hoon, TRPV1-lineage neurons are required for thermal sensation, EMBO J. 30 (2011) 582–593.

[17] L. Karai, D.C. Brown, A.J. Mannes, S.T. Connelly, J. Brown, M. Gandal, O.M. Wellisch, J.K. Neubert, Z. Olah, M.J. Iadarola, Deletion of vanilloid receptor 1-expressing primary afferent neurons for pain control, J. Clin. Invest. 113 (2004) 1344–1352.

[18] G.C. Tender, S. Walbridge, Z. Olah, L. Karai, M. Iadarola, E.H. Oldfield, R.R. Lonser, Selective ablation of nociceptive neurons for elimination of hyperalgesia and neurogenic inflammation, J. Neurosurg. 102 (2005) 522–525.

[19] J.K. Neubert, A.J. Mannes, J. Keller, M. Wexel, M.J. Iadarola, R.M. Caudle, Peripheral targeting of the trigeminal ganglion via the infraorbital foramen as a therapeutic strategy, Brain Res. Brain Res. Protoc. 15 (2005) 119–126.

[20] J.K. Neubert, L. Karai, J.H. Jun, H.S. Kim, Z. Olah, M.J. Iadarola, Peripherally induced resiniferatoxin analgesia, Pain 104 (2003) 219–228.

[21] D.C. Brown, M.J. Iadarola, S.Z. Perkowski, H. Erin, F. Shofer, K.J. Laszlo, Z. Olah, A.J. Mannes, Physiologic and antinociceptive effects of intrathecal resiniferatoxin in a canine bone cancer model, Anesthesiology 103 (2005) 1052–1059.

[22] L. Pecze, W. Blum, B. Schwaller, Mechanism of capsaicin receptor TRPV1-mediated toxicity in pain-sensing neurons focusing on the effects of Na(+)/Ca(2+) fluxes

and the Ca(2 +)-binding protein calretinin, Biochim. Biophys. Acta 1833 (2013) 1680–1691.

[23] M. Naziroglu, I.S. Ovey, Involvement of apoptosis and calcium accumulation through TRPV1 channels in neurobiology of epilepsy, Neuroscience 293 (2015) 55–66.

[24] Z. Olah, T. Szabo, L. Karai, C. Hough, R.D. Fields, R.M. Caudle, P.M. Blumberg, M.J. Iadarola, Ligand-induced dynamic membrane changes and cell deletion conferred by vanilloid receptor 1, J. Biol. Chem. 276 (2001) 11021–11030.

[25] X.X. Dong, Y. Wang, Z.H. Qin, Molecular mechanisms of excitotoxicity and their relevance to pathogenesis of neurodegenerative diseases, Acta Pharmacol. Sin. 30 (2009) 379–387.

[26] R. Sattler, M. Tymianski, Molecular mechanisms of calcium-dependent excitotoxicity, J. Mol. Med. 78 (2000) 3–13.

[27] C. Vercelli, R. Barbero, B. Cuniberti, S. Racca, G. Abbadessa, F. Piccione, G. Re, Transient receptor potential vanilloid 1 expression and functionality in mcf-7 cells: a preliminary investigation, J. Breast Cancer 17 (2014) 332–338.

[28] I. Dhennin-Duthille, M. Gautier, M. Faouzi, A. Guilbert, M. Brevet, D. Vaudry, A. Ahidouch, H. Sevestre, H. Ouadid-Ahidouch, High expression of transient receptor potential channels in human breast cancer epithelial cells and tissues: correlation with pathological parameters, Cell. Physiol. Biochem. 28 (2011) 813–822.

[29] P.A. Kosar, M. Naziroglu, I.S. Ovey, B. Cig, Synergic effects of doxorubicin and melatonin on apoptosis and mitochondrial oxidative stress in MCF-7 breast cancer cells: involvement of TRPV1 channels, J. Membr. Biol. (2015).

[30] G. Czifra, A. Varga, K. Nyeste, R. Marincsak, B.I. Toth, I. Kovacs, L. Kovacs, T. Biro, Increased expressions of cannabinoid receptor-1 and transient receptor potential vanilloid-1 in human prostate carcinoma, J. Cancer Res. Clin. Oncol. 135 (2009) 507–514.

[31] I. Azimi, S.J. Roberts-Thomson, G.R. Monteith, Calcium influx pathways in breast cancer: opportunities for pharmacological intervention, Br. J. Pharmacol. 171 (2014) 945–960.

[32] D. McAndrew, S.J. Roberts-Thomson, G.R. Monteith, TRPV1 and TRPV6 are upregulated in breast cancer cell lines, ComBio 2007 Combined Conference Abstracts. ComBio 2007, Sydney, Australia, 22–26 September 2007, 2007.

[33] L. Pecze, P. Pelsoczi, M. Kecskes, Z. Winter, A. Papp, K. Kaszas, T. Letoha, C. Vizler, Z. Olah, Resiniferatoxin mediated ablation of TRPV1 + neurons removes TRPA1 as well, Can. J. Neurol. Sci. 36 (2009) 234–241.

[34] M. Abdul, S. Ramlal, N. Hoosein, Ryanodine receptor expression correlates with tumor grade in breast cancer, Pathol. Oncol. Res. 14 (2008) 157–160.

[35] H.W. Ai, K.L. Hazelwood, M.W. Davidson, R.E. Campbell, Fluorescent protein FRET pairs for ratiometric imaging of dual biosensors, Nat. Methods 5 (2008) 401–403.

[36] J. Kun, Z. Helyes, A. Perkecz, A. Ban, B. Polgar, J. Szolcsanyi, E. Pinter, Effect of surgical and chemical sensory denervation on non-neural expression of the transient receptor potential vanilloid 1 (TRPV1) receptors in the rat, J. Mol. Neurosci. 48 (2012) 795–803.

[37] C.Y. Park, A. Shcheglovitov, R. Dolmetsch, The CRAC channel activator STIM1 binds and inhibits L-type voltage-gated calcium channels, Science 330 (2010) 101–105.

[38] T.T. Wu, A.A. Peters, P.T. Tan, S.J. Roberts-Thomson, G.R. Monteith, Consequences of activating the calcium-permeable ion channel TRPV1 in breast cancer cells with regulated TRPV1 expression, Cell Calcium 56 (2014) 59–67.

[39] G. Brightwell, V. Poirier, E. Cole, S. Ivins, K.W. Brown, Serum-dependent and cell cycle-dependent expression from a cytomegalovirus-based mammalian expression vector, Gene 194 (1997) 115–123.

[40] C. Larrucea, P. Castro, F.J. Sepulveda, G. Wandersleben, J. Roa, L.G. Aguayo, Sustained increase of Ca + 2 oscillations after chronic TRPV1 receptor activation with capsaicin in cultured spinal neurons, Brain Res. 1218 (2008) 70–76.

[41] F. Touska, L. Marsakova, J. Teisinger, V. Vlachova, A "cute" desensitization of TRPV1, Curr. Pharm. Biotechnol. 12 (2011) 122–129.

[42] M.E. Johansen, C.A. Reilly, G.S. Yost, TRPV1 antagonists elevate cell surface populations of receptor protein and exacerbate TRPV1-mediated toxicities in human lung epithelial cells, Toxicol. Sci. 89 (2006) 278–286.

[43] V. Almendro, A. Marusyk, K. Polyak, Cellular heterogeneity and molecular evolution in cancer, Annu. Rev. Pathol. 8 (2013) 277–302.

[44] T. Yagi, Inhibition by capsaicin of NADH-quinone oxidoreductases is correlated with the presence of energy-coupling site 1 in various organisms, Arch. Biochem. Biophys. 281 (1990) 305–311.

[45] C.A. Reilly, G.S. Yost, Metabolism of capsaicinoids by P450 enzymes: a review of recent findings on reaction mechanisms, bio-activation, and detoxification processes, Drug Metab. Rev. 38 (2006) 685–706.

[46] Y.J. Surh, S.S. Lee, Capsaicin, a double-edged sword: toxicity, metabolism, and chemopreventive potential, Life Sci. 56 (1995) 1845–1855.

[47] Y.M. Kim, J.T. Hwang, D.W. Kwak, Y.K. Lee, O.J. Park, Involvement of AMPK signaling cascade in capsaicin-induced apoptosis of HT-29 colon cancer cells, Ann. N. Y. Acad. Sci. 1095 (2007) 496–503.

[48] C.S. Kim, W.H. Park, J.Y. Park, J.H. Kang, M.O. Kim, T. Kawada, H. Yoo, I.S. Han, R. Yu, Capsaicin, a spicy component of hot pepper, induces apoptosis by activation of the peroxisome proliferator-activated receptor gamma in HT-29 human colon cancer cells, J. Med. Food 7 (2004) 267–273.

[49] S. Rajput, M. Mandal, Antitumor promoting potential of selected phytochemicals derived from spices: a review, Eur. J. Cancer Prev. 21 (2012) 205–215.

[50] S. Singh, K. Natarajan, B.B. Aggarwal, Capsaicin (8-methyl-N-vanillyl-6-nonenamide) is a potent inhibitor of nuclear transcription factor-kappa B activation by diverse agents, J. Immunol. 157 (1996) 4412–4420.

[51] I.S. Ovey, M. Naziroglu, Homocysteine and cytosolic GSH depletion induce apoptosis and oxidative toxicity through cytosolic calcium overload in the hippocampus of aged mice: involvement of TRPM2 and TRPV1 channels, Neuroscience 284 (2015) 225–233.

[52] M. Naziroglu, F.F. Ozkan, S.R. Hapil, V. Ghazizadeh, B. Cig, Epilepsy but not mobile phone frequency (900 MHz) induces apoptosis and calcium entry in hippocampus of epileptic rat: involvement of TRPV1 channels, J. Membr. Biol. 248 (2015) 83–91.

[53] Z. Olah, K. Josvay, L. Pecze, T. Letoha, N. Babai, D. Budai, F. Otvos, S. Szalma, C. Vizler, Anti-calmodulins and tricyclic adjuvants in pain therapy block the TRPV1 channel, PLoS One 2 (2007) e545.

[54] B. Jankovic, D.A. Loblaw, R. Nam, Capsaicin may slow PSA doubling time: case report and literature review, Can. Urol. Assoc. J. 4 (2010) E9–E11 (Journal de l'Association des urologues du Canada).

[55] A. Mori, S. Lehmann, O'Kelly, T. Kumagai, J.C. Desmond, M. Pervan, W.H. McBride, M. Kizaki, H.P. Koeffler, Capsaicin, a component of red peppers, inhibits the growth of androgen-independent, p53 mutant prostate cancer cells, Cancer Res. 66 (2006) 3222–3229.

[56] A.M. Sanchez, M.G. Sanchez, S. Malagarie-Cazenave, N. Olea, I. Diaz-Laviada, Induction of apoptosis in prostate tumor PC-3 cells and inhibition of xenograft prostate tumor growth by the vanilloid capsaicin, Apoptosis 11 (2006) 89–99.

[57] T.D. Tlsty, L.M. Coussens, Tumor stroma and regulation of cancer development, Annu. Rev. Pathol. 1 (2006) 119–150.

[58] S. Li, Y. Sun, D. Gao, Role of the nervous system in cancer metastasis, Oncol. Lett. 5 (2013) 1101–1111.

[59] S.A. Spindler, F.H. Sarkar, W.A. Sakr, M.L. Blackburn, A.W. Bull, M. LaGattuta, R.G. Reddy, Production of 13-hydroxyoctadecadienoic acid (13-HODE) by prostate tumors and cell lines, Biochem. Biophys. Res. Commun. 239 (1997) 775–781.

[60] A. Alexanian, A. Sorokin, Targeting 20-HETE producing enzymes in cancer — rationale, pharmacology, and clinical potential, OncoTargets Ther. 6 (2013) 243–255.

[61] J. Szolcsanyi, Capsaicin and sensory neurones: a historical perspective, Prog. Drug Res. 68 (2014) 1–37 (Fortschritte der Arzneimittelforschung. Progres des recherches pharmaceutiques).

[62] K. Ondicova, B. Mravec, Role of nervous system in cancer aetiopathogenesis, Lancet Oncol. 11 (2010) 596–601.